Journal of Non-Crystalline Solids 612 (2023) 122337

Contents lists available at ScienceDirect

Journal of Non-Crystalline Solids

journal homepage: www.elsevier.com/locate/jnoncrysol

Effect of thermal treatment on ZnSe quantum dots and energy transfer in borosilicate glasses doped with ZnSe and Er^{3+}/ZnSe

Nilanjana Shasmal [a,*], Andrea Simone Stucchi de Camargo [b], Ana Candida Martins Rodrigues [a]

[a] Federal University of São Carlos, Department of Materials Engineering, LaMaV - Laboratório de Materiais Vítreos, Rod. Washington Luiz, km 235, 13565-905, São Carlos, SP, Brazil

[b] University of São Paulo, São Carlos Institute of Physics, LEMAF – Laboratório de Espectroscopia de Materiais Funcionais, Avenida Trabalhador São-carlense, n° 400 Parque Arnold Schimidt - CEP 13566-590, São Carlos, SP, Brazil

ARTICLE INFO

Keywords:
ZnSe quantum dots
ZnSe/Er^{3+} co-doped glass
Erbium-doped glass
Energy transfer

ABSTRACT

This study assessed the effect of heat treatment on the spectroscopic properties of borosilicate glasses doped with ZnSe quantum dots (QDs) and co-doped with Er^{3+}/ZnSe. The gradual growth of ZnSe QDs upon heat treatment was probed by TEM. The emission intensity of ZnSe-doped glasses rapidly increased up to 20 h of heat treatment because of the formation and development of ZnSe QDs, then gradually decreased due to the rise in non-radiative loss between the enlarged particles. With increasing number of ZnSe QDs, the energy transfer from QDs to Er^{3+} ions became prominent in Er^{3+}/ZnSe-co-doped glasses, showing enhanced emission up to 20 h of heat treatment. The excited state $^4S_{3/2}$ lifetime values, increased with heat treatment, whereas an opposite trend was observed for the lifetime values of state $^4I_{13/2}$, indicating a possible participation of the ZnSe QDs in facilitating the energy migration mechanism through the $^4I_{13/2}$ level, followed by non-radiative decay.

1. Introduction

Semiconductor quantum dots (QDs) with sizes comparable to the Bohr exciton radius show unique size-dependent optical properties due to quantum confinement effects, drawing significant research interest over the past two decades [1–3]. The downsizing of the particles causes the discretization of the energy levels. Depending on the size of the QDs, the semiconductor bandgap differs, allowing tunable optical properties [4–7]. Especially, the II-VI semiconductors (CdS, ZnS, ZnTe, CdSe, ZnSe, etc.), within the size range of 1–100 nm, show intense response to the size-dependent properties [8]. Zinc selenide was one of the first discovered II-VI semiconductors with wide-bandgap which has become a very important electronic and optoelectronic material, with eminent applications in nonlinear optical devices like lasers, light-emitting diodes (LEDs), flat-panel displays, transistors, logic gates, etc. Recently, ZnSe nanostructures have attracted much interest for its promising applications in both fundamental physical research and in the fabrication of nanoscale electronic and optoelectronic devices [9].

The synthesis and spectroscopic characterization of ZnSe QDs have been reported by several authors [10–16]. These QDs exhibit a broadband red emission originating from size-related electron-hole recombination and emissions from defects to traps resulting from Se and Zn vacancies [10–16]. Co-doping of semiconductor and rare earth in different glass matrices has also been described in the existing literature. For instance, the spectroscopic investigation of Eu^{3+} ions in silica glasses embedded with CdSe nanocrystals showed that the CdSe nanocrystals instigate an intensity enhancement of Eu^{3+} emissions through energy transfer [17]. Enhancement in Eu^{3+} emissions were also witnessed by a similar kind of energy transfer from ZnO QDs [18] or ZnSe nanocrystals embedded in SiO_2 glass [19], as well as in the presence of ZnO, SnO_2 [20] and ZnSe nanocrystals in silica hosts [19]. Almost identical mechanisms of energy transfer have been observed for CdS/Nd^{3+} [21], CdS/Er^{3+} [22,23], ZnSe/Er^{3+} [24] and CdS/Eu^{3+} [25] co-doped systems.

Given the above and in search for the evolution of new materials with enhanced luminescent properties, we recently reported the synthesis and spectroscopic characterization of borosilicate glasses co-doped with different concentrations of Er^{3+} and ZnSe, which revealed a significant enhancement in Er^{3+} emissions due to effective energy transfer from ZnSe QDs to Er^{3+} ions [24]. In the present study, we investigated the effect of an optimized thermal treatment protocol on the energy transfer process in these previously Er^{3+} doped and Er^{3+}/ZnSe co-doped glasses. The sizes of the ZnSe QDs in the glasses with different ZnSe concentrations were probed as a function of heat treatment duration.

* Corresponding author.
E-mail address: nilanjana@ufscar.br (N. Shasmal).

https://doi.org/10.1016/j.jnoncrysol.2023.122337
Received 26 January 2023; Received in revised form 12 March 2023; Accepted 12 April 2023
Available online 26 April 2023

Morphological studies were conducted by microscopic techniques like transmission electron microscopy (TEM) and energy dispersive X-Ray (EDX) measurements. Spectroscopic characterization was carried out by UV–*Vis* absorption and photoluminescence (PL) spectroscopy analyses.

2. Experimental procedure

2.1. Preparation

Borosilicate glasses with base composition $42SiO_2$–$30B_2O_3$–20BaO-$4K_2O$-$4Al_2O_3$ were prepared by a conventional one-step melt-quenching technique, in a 60 g batch. This composition was chosen based on our previous studies that showed it to be an excellent host for ZnSe and ZnSe/Er^{3+} doping [24]. The raw materials used in the synthesis, as well as melting and annealing procedure are described in our previous work [24]. The compositions of all samples are shown in Table 1. ZnSe and Er_2O_3 were added in excess.

2.2. Characterization

Microstructures were investigated by TEM and EDX on a SEM XL30 FEG microscope. XRD measurements of the powders was executed with a Rigaku Ultima IV diffractometer using Cu-K_α radiation in the interval of $2\theta = 10$–80°, with a step of 0.1° and 1 s counting time. For the investigation of spectroscopic properties, each sample was cut into sections with the same dimensions (15 mm X 15 mm X 5 mm) and polished. The absorption spectra was recorded with a UV–*Vis*-NIR spectrophotometer (Perkin-Elmer Lambda 950). The excitation and emission spectra were collected on a spectrofluorometer (HORIBA Jobin Yvon, model Fluorolog FL3–221), equipped with a CW xenon flash lamp and a photomultiplier detector (HORIBA, PPD-850). The excitation wavelength selection from the broadband lamp emission was achieved by optical gratings. Regarding the discussions based on relative PL intensity, we emphasize that since the intensity scales of commercial equipments are usually not calibrated, we are only referring to trends and not making quantitative strict comparisons. In order to do so, besides assuring that all the samples had the same dimensions, they were placed and measured in the same positions, to the best of our experimental control.

2.3. Heat treatment

The glass containing 0.6 wt% ZnSe was subjected to differential scanning calorimetry (DSC) on a DSC-Netzsch 404 equipment. The glass transition temperature (T_g) was found at ~600 °C [24]. All the glasses were heat treated at 650 °C. To confirm the uniformity of the results, the same glass samples were heat treated for accumulative times, from 10 min to 60 h. Then, they were placed in the spectrofluorometer, for each measurement, at the exact same position. Fig. 1 shows the photographs of some as-prepared and heat-treated glasses. All the heat-treated glasses maintain their transparency during the whole course of the experiments i.e. up to 60 h of heat treatment. The ZnSe-doped glasses get darker with heat treatment indicating generation of an increasing number of ZnSe QDs.

Table 1
Composition and resulting color of the prepared glasses.

Sample no.	Sample ID	ZnSe content (wt %, in excess)	Er_2O_3 content (wt %, in excess)	Color
1	ZnSe06	0.6	–	Brown
2	ZnSe08	0.8	–	Brown
3	ZnSe10	1.0	–	Brown
4	Er15	–	1.5	Pink
5	Er15_ZnSe06	0.6	1.5	Purple
6	Er15_ZnSe08	0.8	1.5	Purple
7	Er15_ZnSe010	1.0	1.5	Purple

Base glass composition: $42SiO_2$–$30B_2O_3$–20BaO-$4K_2O$-$4Al_2O_3$.

3. Results and discussion

3.1. X-ray diffraction

X-ray diffraction analysis was conducted for all the as-prepared and heat-treated samples. Fig. 2 shows, representative XRD patterns of the heat-treated glasses. The halo between $2\theta = 20^\circ$-35° in all the patterns, and the absence of any distinguishable peaks, evidences the amorphous nature of the samples. In other words, none of the glass samples exhibit any sign of crystallization, even after being subjected to the longest heat treatment time.

3.2. Transmission electron microscopy (TEM)

3.2.1. ZnSe06 sample

Fig. 3(a) and (b) show the TEM images of the as-prepared ZnSe06 sample. Small particles (average size < 10 nm) can be clearly seen distributed over the glass matrix; however, very few particles with smaller average size (< 2 nm) are observed. All the particles seem to be spherical in shape. Fig. 3(c) and (d) show the transmission electron microscopy images of ZnSe06 sample heat treated for 40 h at the same temperature, with relatively larger particles, in the 30–50 nm size range. Fig. 3(e) and (f) show the TEM images of an additional ZnSe06 sample heat treated for 60 h. As expected, the particles have grown larger than those observed after 40 h of heat treatment, with an average size higher than 100 nm. The particle shown in Fig. 3(f) is ~300 nm in diameter. Both smaller (~100 nm) and larger (~300 nm) particles can be observed.

EDX analysis was also conducted for all the heat-treated samples. Fig. 4 shows the EDX spectrum of a selected area (inset) of the ZnSe06 sample, heat treated at 650 °C for 60 h. As evident, it proves the existence of both Zn and Se in the sample. The weight percentages of all the constituent elements are shown in Table 2. Presence of Zn and Se in significant amount, is a solid evidence that the particles are constituted of ZnSe QDs.

3.2.2. Co-doped Er15_ZnSe06 sample

Fig. 5 shows the TEM images of the E15_ZnSe06 co-doped sample heat treated for 20, 40 and 60 h at 650 °C. After 20 h of heat treatment, minute particles (mean size <10 nm) are observed, as shown in Fig. 5(a) and (b). After 40 h, both smaller and larger particles, in the range of 20–60 nm, can be seen, as shown in Fig. 5(c) and (d). In addition, the number of particles is visibly greater, suggesting that new particles are formed and the previously existing ones grow larger with prolonged heat treatment, resulting in a wide size distribution. The same phenomenon was observed after 60 h of heat treatment, as shown in Fig. 5(e) and (f). A large number of particles in a wide size range (10–100 nm) can be observed, forming an agglomerate.

EDX spectra have been measured for each sample to determine the chemical composition of the particles. All of them show practically the same result, confirming that the particles constitute of ZnSe. Fig. 6 shows representative EDX spectra of a selected area (inset) of the 40 h heat treated E15_ZnSe06 sample. The EDX quantitative analysis of the selected area is shown in Table 3.

3.3. Absorption spectra of heat-treated samples

Very small particles were detected by TEM in the ZnSe06 sample, as shown in Fig. 3(a) and (b). These particles become larger with increasing heat treatment duration: from ≤ 10 nm in the as-prepared glasses to 30–50 nm after 40 h and >100 nm after 60 h of heat treatment, Fig. 3 (c-f). The effect of this enlargement was observed in the UV–*Vis* absorption spectra, as shown in Fig. 7(a). Broad absorption bands, observed around 367, 498 and 760 nm, indicate the presence of ZnSe quantum dots of

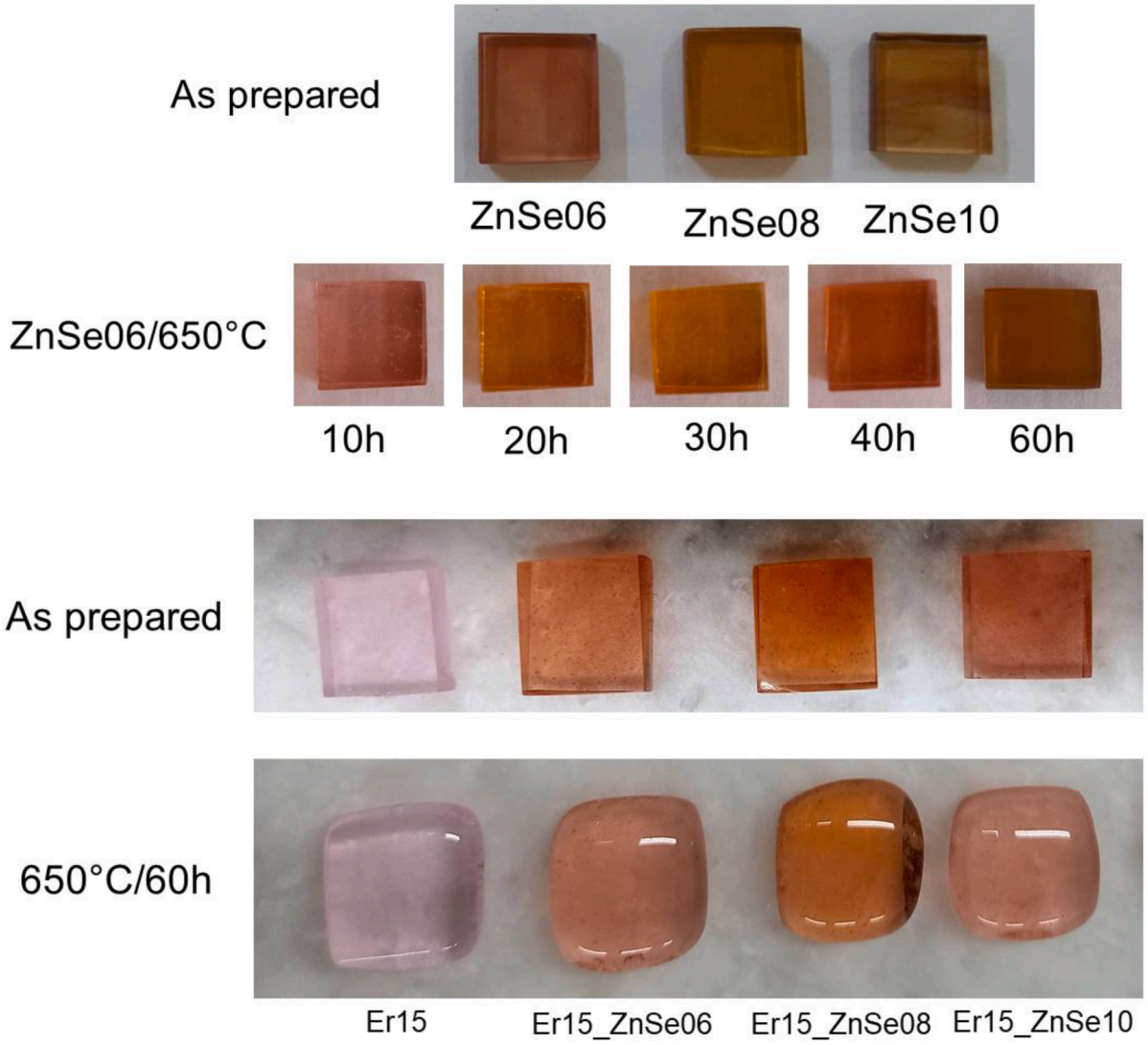

Fig 1. Examples of some as prepared and heat-treated glasses.

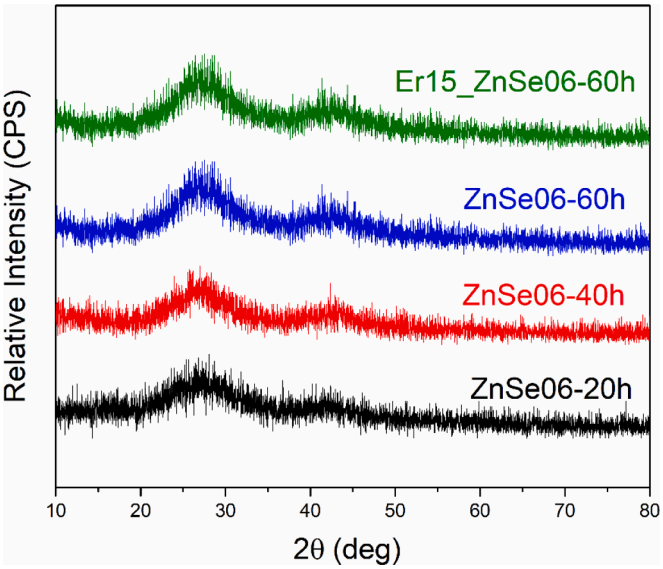

Fig 2. Representative XRD patterns of heat-treated samples.

different sizes. The band at 367 nm is the most prominent one and indicates that most of the ZnSe QDs generated in the glass, are of smaller sizes [8,16,24,26,27]. The other lower intensity bands at higher wavelengths, indicate the formation of fewer QDs of larger sizes. The broadness and intensities of all the bands rise slightly with increasing heat treatment duration because of the formation of new ZnSe QDs as well as the growth of already existing QDs [24,26,27]. All other ZnSe-doped glasses show the same behavior upon heat treatment.

A similar absorption variation trend was observed in the case of Er^{3+}/ZnSe co-doped glasses. Fig. 7(b) shows the UV–*Vis* absorption spectra of the E15_ZnSe06 sample heat treated at 650 °C for different times. The absorption spectra exhibit the signatures of both the optically active ingredients present in the glass – ZnSe QDs and Er^{3+} ions. For example, both the absorption bands from Er^{3+} and ZnSe overlap with each other around 500 nm. Around 360–380 nm, the sharp absorption peaks of Er^{3+} at 377 nm are quite distinguishable, accompanied by the broad band of ZnSe. Quite predictably, this broad bands gets more and more prominent with increasing ZnSe content. All the other co-doped samples display the same absorption features.

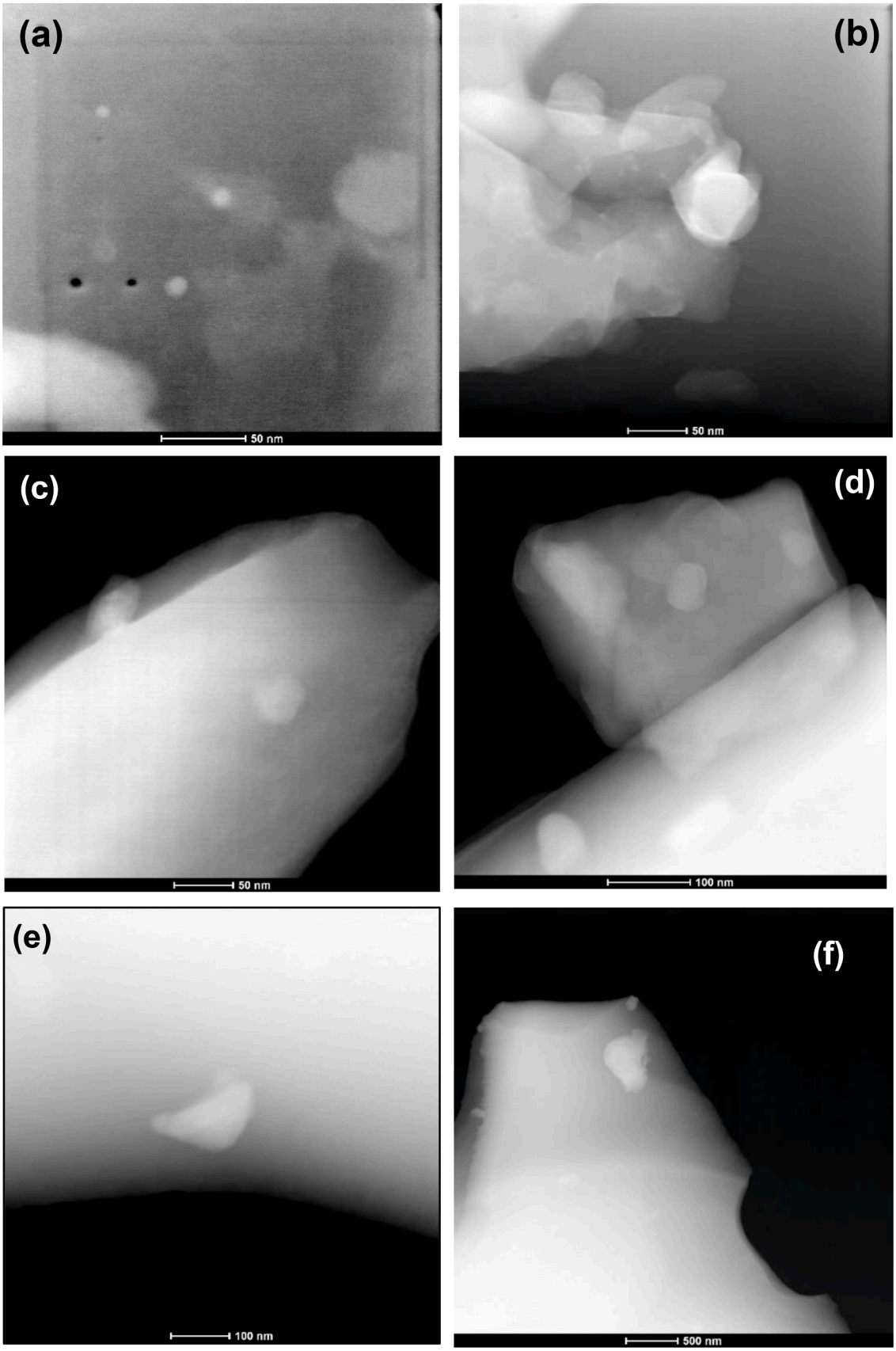

Fig 3. TEM images of the as-prepared ZnSe06 glass sample: (a) and (b), and the ZnSe06 sample heat treated at 650 °C for (c) 20 h, (d) 40 h, and (e) and (f) 60 h.

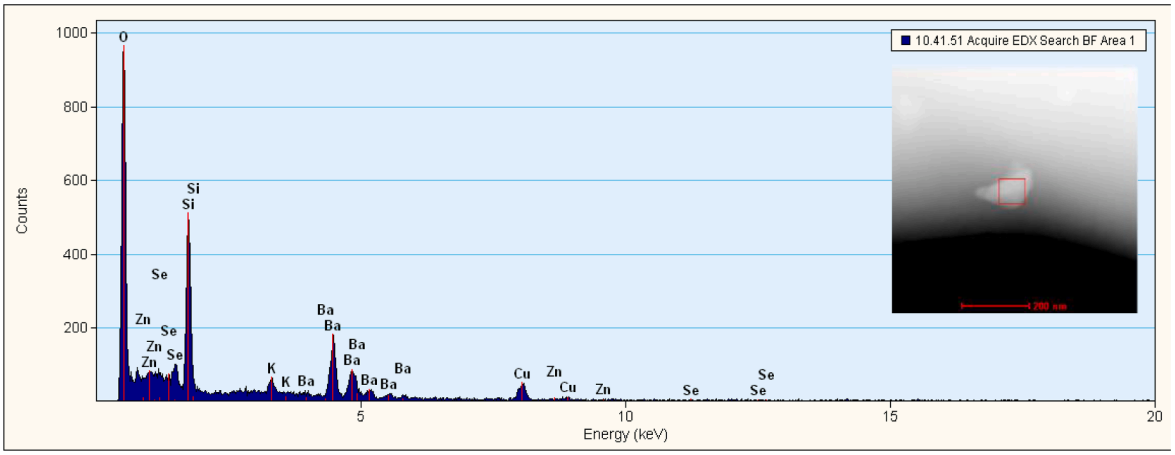

Fig. 4. EDX spectra of a selected area (inset) of the ZnSe06 sample heat treated at 650 °C for 60 h.

Table 2
EDX quantitative analysis of a selected area [as shown in Fig. 4] of the ZnSe06 sample heat treated at 650 °C for 20 h.

Element	Weight%	Atomic%	Uncert.%
O(K)	56.23	77.57	0.53
Al(K)	6.49	5.31	0.13
Si(K)	17.66	13.83	0.20
Zn(K)	0.41	0.12	0.03
Se(K)	0.49	0.13	0.03
Ba(K)	18.96	3.04	0.48

3.4. Emission spectra of heat-treated samples

3.4.1. Heat treated ZnSe-doped glasses

The effect of heat treatment at 650 °C for several time durations (10 min to 60 h) on the PL emission of ZnSe06 samples was analyzed. Fig. 8 (a) shows the resulting PL emission spectra upon excitation at 367 nm. The variation trend is the same for excitation at 498 nm (Fig. S1 in the Supplementary Material). In both cases, characteristic broad emission band peaks are observed around 700 nm. The appearance of the broad multiple-band structure can be attributed to the overlapping emissions from the ZnSe QDs (originating from electron-hole recombination) and transitions from defect states to trap states (originating from Se and Zn vacancies) [8,16,24]. Bright red luminescence was observed in all heat-treated samples. Intensity varied considerably with the duration of heat treatment.

Fig. 9(a) shows the variation of maximum PL intensity at 367 nm with respect to heat treatment duration. The PL intensity shows an initial sharp increase up to 1 h of heat-treatment, followed by a smoother increase up to 20 h, and then a steady decrease. The initial sharp emission intensity increase is attributed to the formation of new ZnSe NPs, as well as to the growth of the previously existing NPs over the heat treatment. Formation of new particles in a glass matrix while heat treated above the glass transition temperature is a well-known phenomenon. In this glass, minute ZnSe QDs begin to form at elevated temperature during the heat treatment. These small QDs contribute to the overall PL emission of the glass, leading to the steep increase in PL intensity up to a certain heat treatment time (2 h in this case). After that, the rate of formation of ZnSe QDs slows down and the existing particles continue to grow, which leads to a slow increase in PL intensity. Eventually, it reaches a maximum level where the enhancement effect of the QDs emission is at its maximum (20 h for this sample). After that, crowding of the glass matrix with larger QDs results in decreased interparticle distance and the overall emission intensity decreases due to increased non-radiative relaxation among the ZnSe QDs, leading to reduced radiative emission intensity.

As an expected effect of the QDs growth, the peak of the broad emission band shows a gradual red-shift with increasing duration of heat treatment (Fig. 9(b)). For shorter heat treatment times, the change in peak position is sharp, whereas it shows a gradual and almost linear red shift of the peak after 10 h of heat treatment. This shift depends on the QDs growth dynamics in a similar way to what is observed in Fig. 9(a). Increasing heat treatment duration leads to, first, an elevated rate of precipitation accompanied and followed by an enlargement of the dots. The increase in particle size leads to a gradual decrease of the energy gap between the valence band (VB) and the conduction band (CB) which explains the red shift of the peak position. The same behavior of PL intensity and peak positions was observed for heat-treated glasses excited at 498 nm, as shown in Fig. S2 (a) and (b).

The glasses with different ZnSe content (0.8 and 1.0 wt%, in excess) showed a similar trend of PL intensity variation when undergoing the same heat treatment. Fig. 10(a) and (b) show the variation of maximum PL intensity of the 700 nm band in the ZnSe-doped glasses with heat treatment duration. The rate of PL enhancement changed proportionally to ZnSe content. The highest PL enhancement was observed for the sample with the largest ZnSe content (1.0 wt%), given the larger number of ZnSe QDs formed at the beginning of heat treatment. The larger the number of smaller ZnSe particles, the greater the contribution to the overall emission. The saturation point appears around the same heat treatment duration (20 h) for all the samples. For the ZnSe10 sample excited at 367 nm, the enhancement from 10 to 20 h is notably lower than those for the other samples, probably due to the higher concentration of ZnSe, which attains the favorable size and number of QDs earlier than for the other samples. Similar trends in PL intensity and energy shifting have been previously reported for glasses doped with ZnSe [16] and other II-VI semiconductor dots as CdSe [28] and CdS [29, 30].

3.4.2. Er^{3+}/ZnSe co-doped glasses

3.4.2.1. Emission spectra in the visible region. The PL spectra of heat-treated co-doped glasses at 377 nm excitation present both the characteristic emission bands of Er^{3+} (at 546 nm, $^4S_{3/2} \rightarrow {}^4I_{15/2}$ transition) and ZnSe (broadband centered at ~ 700 nm), as shown in Fig. 11. Fig. 11(a) shows the PL spectra of the Er15_ZnSe06 sample heat treated at 650 °C for different times. The emission spectra of all the co-doped glasses present similar variation trend (Fig. S3). In Fig. 11(b) it is clearly noted that for all the co-doped samples, the Er^{3+} emission in the green (546 nm) presents higher intensity than for the Er15 sample doped only with Er^{3+}. The reason for that lies in the presence of QD → Er^{3+} energy transfer, as previously reported by us and other authors [18–24]. In our previous work [24], a spectroscopic study has been carried out on the

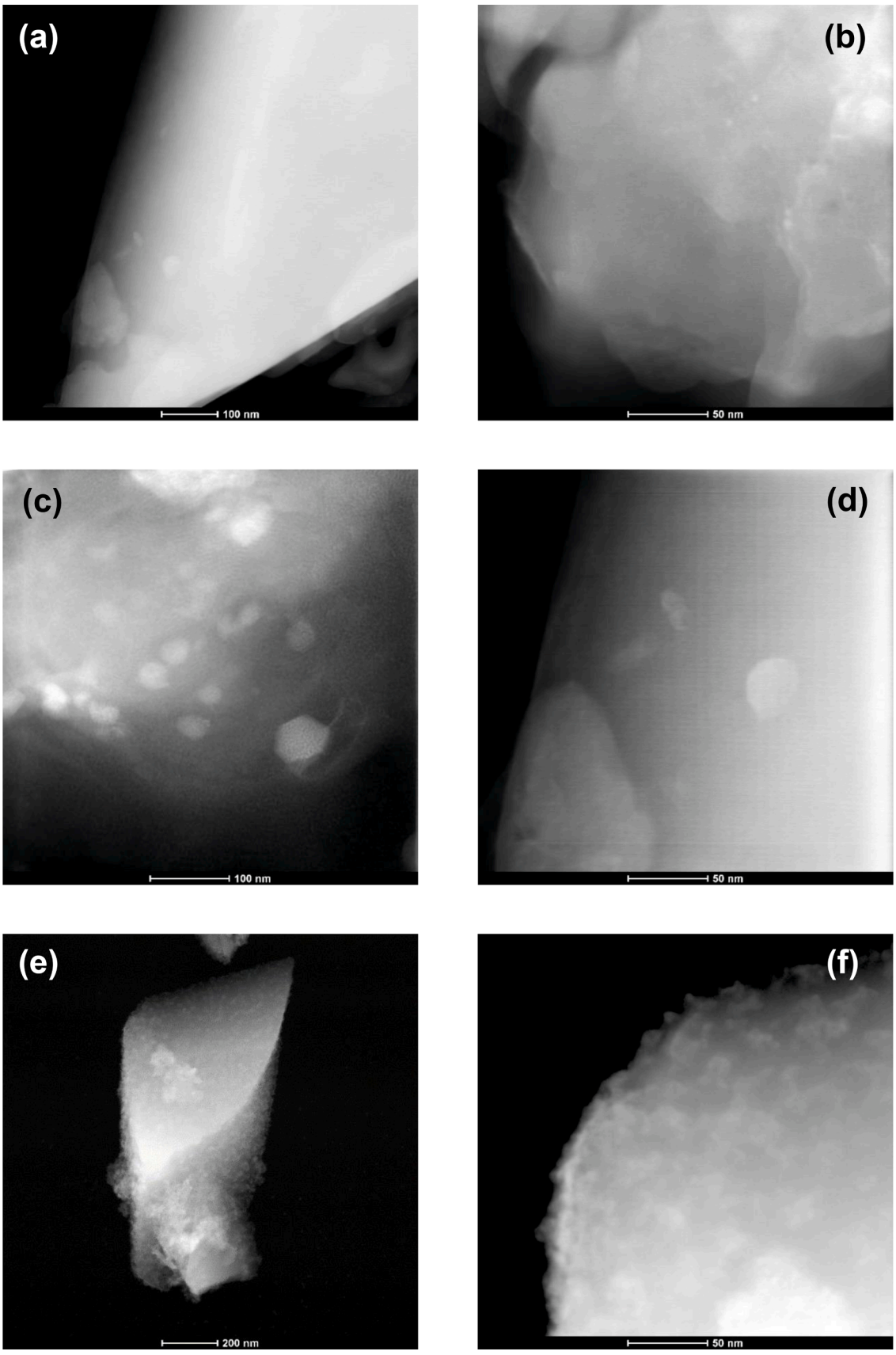

Fig. 5. TEM images of the E15_ZnSe06 sample heat treated at 650 °C (a) and (b) 20 h, (c) and (d) 40 h, and (e) and (f) 60 h.

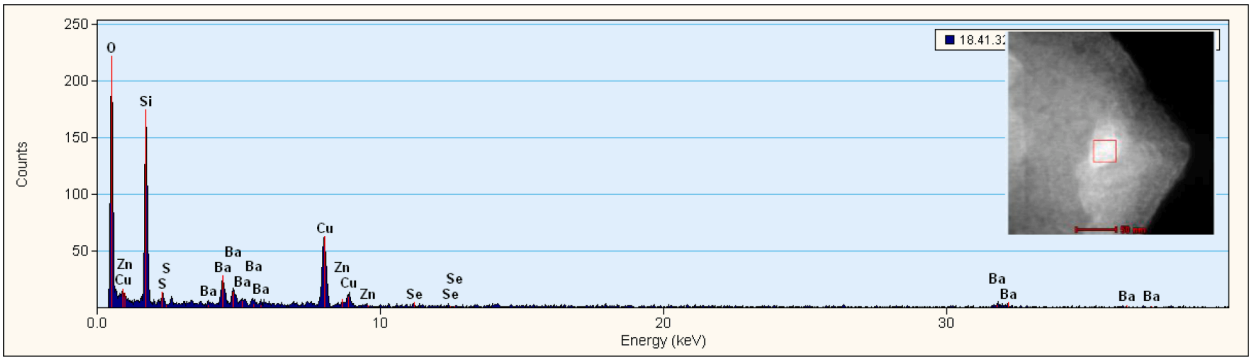

Fig 6. EDX spectra of a specific area (inset) of the E15_ZnSe06 sample heat treated for 40 h at 650 °C.

Table 3
EDX quantitative analysis of a specific area [Fig 6, inset] of E15_ZnSe06 heat-treated for 40hs at 650 °C.

Element	Weight%	Atomic%	Uncert.%
O(K)	61.22	78.94	1.58
Si(K)	25.03	18.38	0.72
Al (K)	1.12	0.72	0.17
Zn(K)	0.13	0.04	0.20
Se(K)	0.27	0.07	0.28
Ba(K)	12.21	1.83	2.74

Er^{3+}/ZnSe co-doped glasses. Several evidences of energy transfer from excitation and emission spectra, have been explained in detail. The mechanism of energy transfer has also been previously described [24]. The spectral intensity variation in the green region in both parts (a) and (b) clearly shows that the effect of the energy transfer is favored by increasing the heat treatment of the co-doped samples from 0 to 20 h, given the increasing growth of QDs. However, for heat treatment times higher than 30 h, a progressive decrease in the green emission is observed. As a hypothesis, we argue that the larger sized QDs formed at these conditions undergo prominent non-radiative energy decay (radiation damping effect [21–23]), thus contributing less to the transfer to Er^{3+}. The assumption is corroborated by the similar intensity trend of the red emission (~700 nm) of the ZnSe QDs for both cases, of ZnSe-doped glasses (Figs. 9 and 10), and for co-doped glasses (Fig. 11 (a)). In this last case, we assume that the intensity variation between the non-heated sample and the one heat treated at 10 h, is practically the same, within experimental error.

When comparing the Er^{3+} green emission intensity trends among the different co-doped samples, subjected to the same heat treatment conditions (Fig. 11(b)) similar trends are seen. There is clear indication that the heat treatment time of 20 h, among those investigated, is indeed the optimum condition to prepare glasses with increased Er^{3+} and ZnSe QDs emissions. It is also observed that the rate of PL intensity decrease is much higher in the Er15_ZnSe10 glass containing the highest concentration of ZnSe. This is also expected as the radiation damping effect is more pronounced after reaching the maximum PL intensity.

3.4.2.2. Emissions in the IR region. The emission of the glasses were also measured in the IR spectral range upon 377 nm excitation. The intensity variation trend was the same as that observed in the visible region, as shown in Fig. 12. Fig 12(b) shows the variation in PL intensity of the Er15_ZnSe06 sample for different heat treatment durations. All the other co-doped glasses show a similar variation (Fig S4). The PL intensities reach their maximum after 20 h of heat treatment and the observed PL enhancement rises with the increase in ZnSe content. Maximum enhancement was observed for the glass with 1.0 wt% ZnSe after 20 h of heat treatment, both in the green and IR emissions. A maximum 5-fold intensity enhancement was observed for the Er15_ZnSe10 sample at

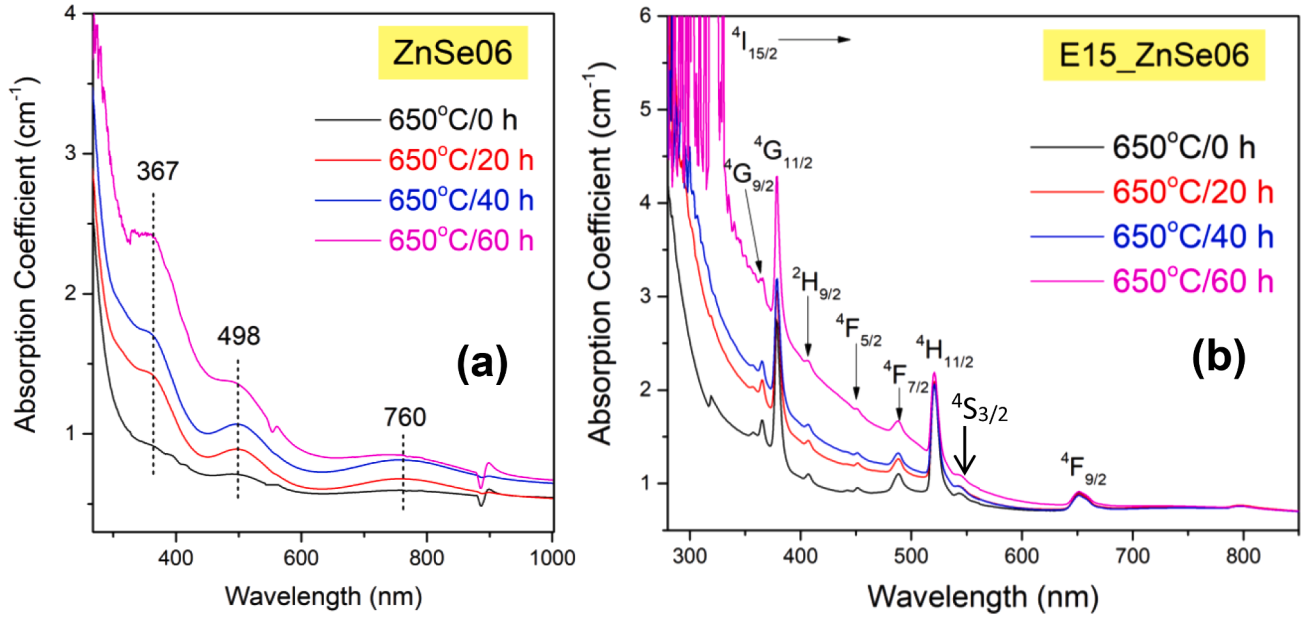

Fig. 7. UV–Vis absorption spectra of (a) ZnSe06 sample and (b) E15_ZnSe sample heat-treated at indicated times at 650 °C.

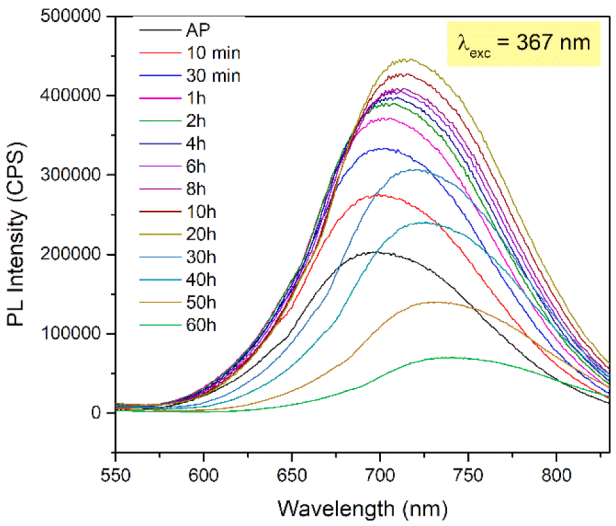

Fig. 8. PL emission spectra at 367 nm excitation, of ZnSe06 sample heat-treated at increasing periods of time.

1533 nm ($^4I_{13/2} \rightarrow {}^4I_{15/2}$ transition), while the 546 nm emission enhanced 2.5-fold.

3.5. Fluorescence lifetimes

For heat-treated Er^{3+}/ZnSe co-doped glasses, the fluorescence lifetimes were estimated by monitoring the emissions at 550 and 1533 nm, upon excitation at 377 nm. Fig. 13(a) and (b) show the variation in lifetime values, as a function of heat treatment duration. For the emission at 550 nm, the lifetime values of the emitting level $^4S_{3/2}$ increase with heat treatment. This effect is not due to an intrinsic increase of Er^{3+} emission probability but, rather, due to the increased energy transfer probability from the ZnSe QDs, as previously discussed. The energy transfer thus constitutes an additional excitation channel to Er^{3+} ions leading to an apparent (measurable) increase in lifetime values. On the contrary, the variation of lifetime values in the infrared ($^4I_{13/2}$ level) goes in the opposite direction, that is, with increasing ZnSe content and heat treatment times, there is a slight decrease (10–15%) in lifetime values. Because at this Er^{3+}doping concentration (1.5 wt%) the emitting level $^4I_{13/2}$ is prone to energy migration followed by non-radiative energy loss to defects, it can be reasonably argued that the presence of the ZnSe QDs might play a role in facilitating the migration in co-doped samples, as compared to the singly doped Er15 sample. However, proof of this hypothesis can only be given through a dedicated study that should include the measurement of lifetimes of ZnSe QDs in the co-

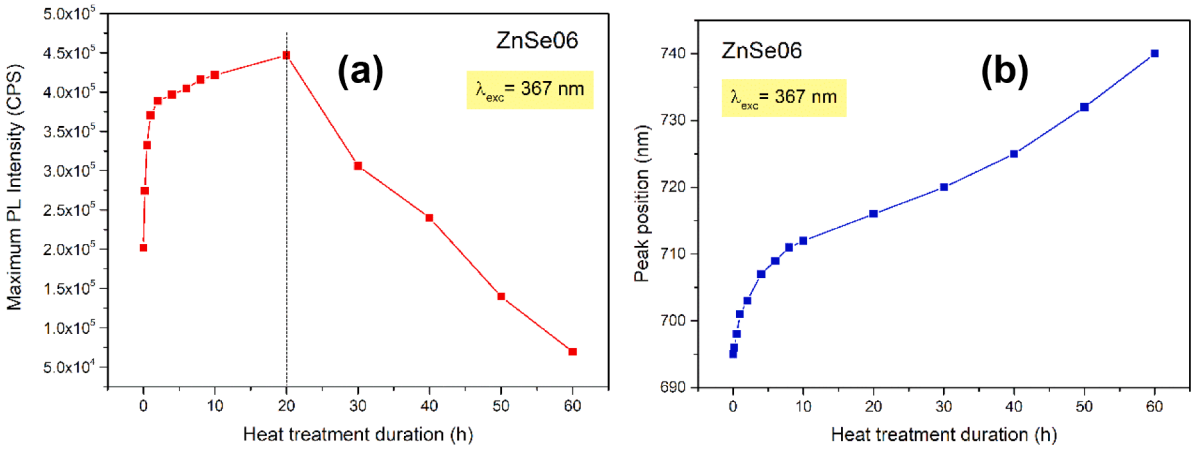

Fig. 9. Variation of (a) maximum PL intensity at peak position and (b) peak position of ZnSe06 at 367 nm excitation, both with heat treatment duration.

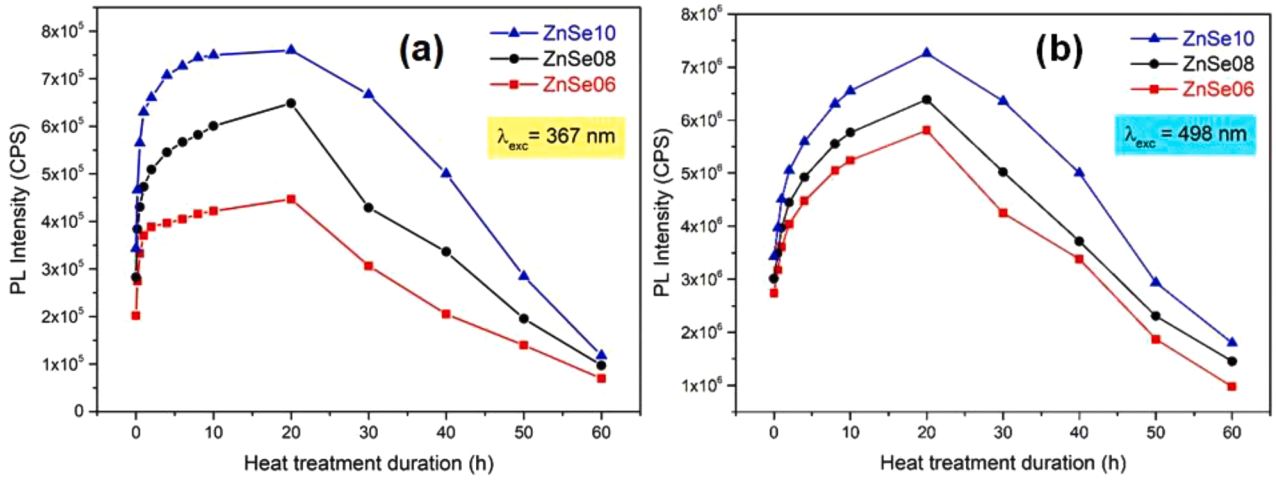

Fig. 10. Maximum PL intensity around 700 nm, for glasses containing different concentrations of ZnSe, as a function of heat-treatment duration, excited at (a) λ_{exc}= 367 nm and (b) λ_{exc}= 498 nm.

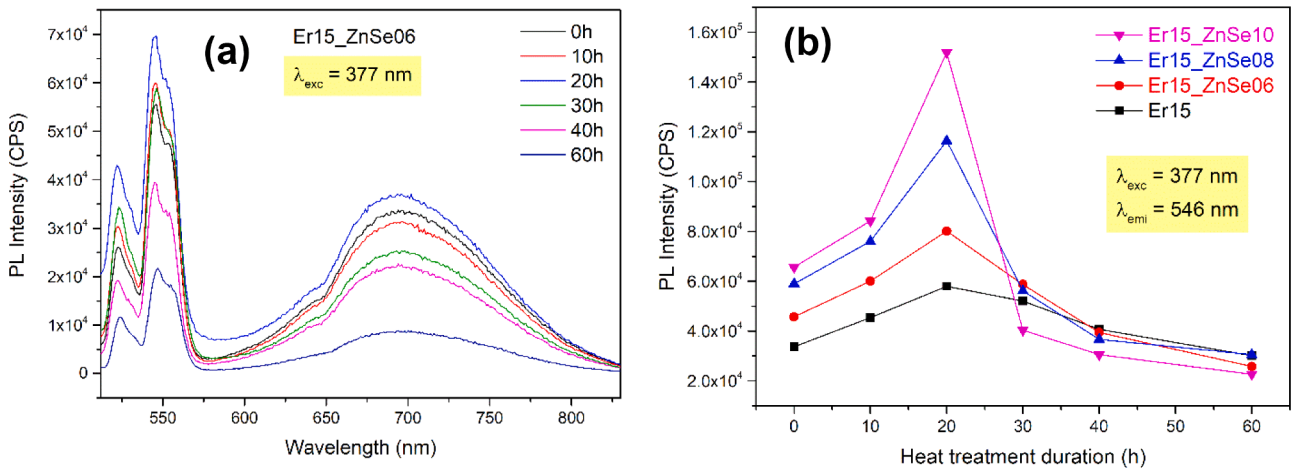

Fig. 11. (a) PL emission spectra of the Er15_ZnSe06 sample excited at 377 nm for indicated heat-treatment durations at 650 °C and (b) PL intensity for Er^{3+}-doped and Er^{3+}/ZnSe co-doped glasses at 546 nm with heat treatment duration.

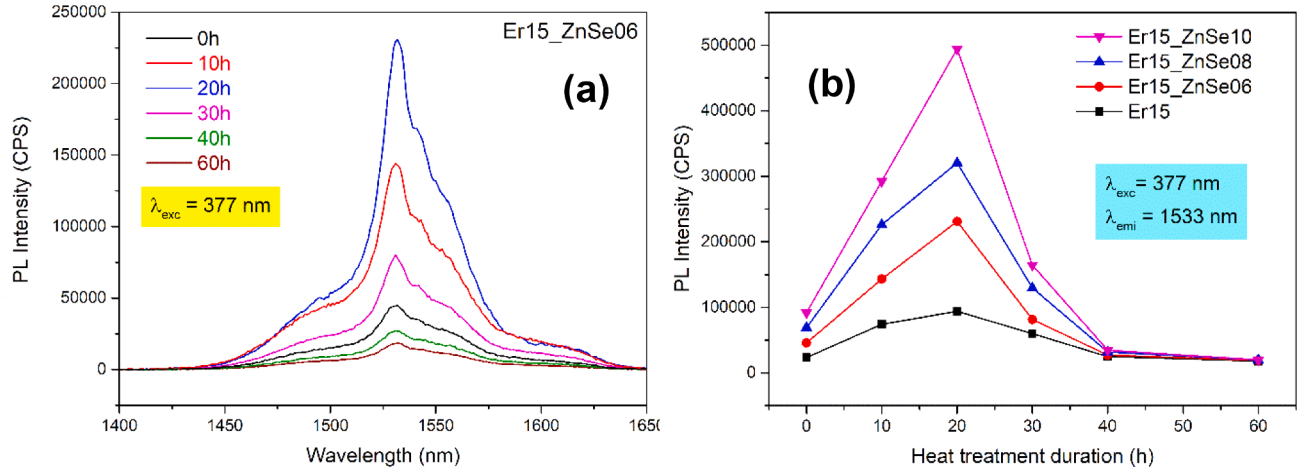

Fig. 12. (a) PL emission spectra of Er15_ZnSe06 in the IR region at 377 nm excitation as a function of indicated heat-treatment duration and (b) PL intensity of the Er^{3+}-doped and Er^{3+}/ZnSe co-doped glasses at 1533 nm with varying heat-treatment duration.

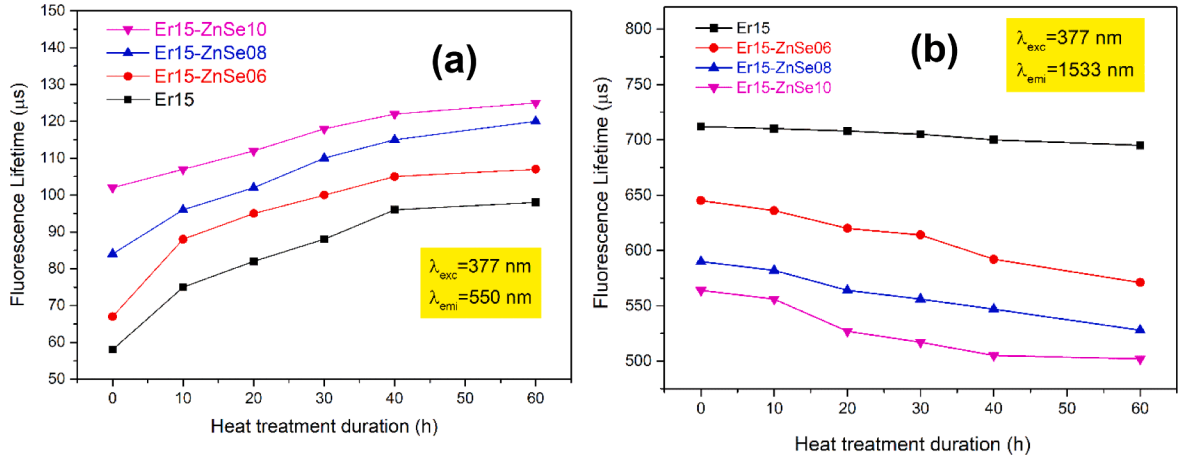

Fig. 13. Fluorescence lifetimes of Er^{3+}-doped and Er^{3+}/ZnSe co-doped glasses containing different concentrations of ZnSe for (a) emission at 550 nm and (b) at 1533 nm with heat treatment duration.

doped and singly doped samples, and possibly transient absorption measurements. Unfortunately, we were not able to measure the ZnSe QDs lifetimes, due to equipment (timespan) limitations. Because this fact does not absolutely invalidate the results and discussions presented in this contribution, we plan to conduct a further, future investigation in that direction.

4. Conclusions

ZnSe-doped and Er^{3+}/ZnSe co-doped borosilicate glasses were heat treated for different times up to 60 h at 650 °C to investigate their optical and spectroscopic properties, especially with respect to QD → Er^{3+} energy transfer, leading to Er^{3+} emission intensity increase. XRD patterns revealed that the glasses do not crystallize within the experimental range of heat treatment. TEM and EDX studies confirmed the formation of ZnSe QDs of size range <10 nm in the as-prepared glasses, which formed during the glass preparation steps. With increasing heat treatment duration, enlargement of previously existing QDs and generation of new QDs were observed. The steady broadening of the absorption bands emerging from ZnSe also confirmed the enlargement of the QDs with heat treatment. PL emission from ZnSe-doped glasses rapidly increased up to 20 h of heat treatment because of the generation and growth of QDs, and then gradually decreased as a result of the rise in non-radiative loss between the enlarged particles. As a consequence of the enlargement of ZnSe QDs, effective band gap decrease led to the red shift of the particles' emission peaked around 700 nm. Er^{3+}/ZnSe co-doped glasses showed the same variation trend in PL intensities as observed in ZnSe-doped glasses. With the increasing number of ZnSe QDs, the energy transfers from ZnSe to Er^{3+} ions (proved and explained in details earlier in our previous work [24]) became more prominent, resulting in enhanced emission for samples heat-treated up to 20 h. For higher heat treatment times, further growth of ZnSe QDs results in decreased PL intensity. These observations apply to both the visible and near-infrared emissions of Er^{3+}. Maximum enhancement (5-fold) of the 1530 nm emission was observed for the sample with highest ZnSe concentration (1 wt%) while the emission at 546 nm showed a 2.5-fold intensity increase. Fluorescence lifetime values were measured for the $^4S_{3/2}$ and $^3I_{13/2}$ levels of Er^{3+} in the visible and near-infrared. In the case of the visible emission, an apparent increase of the values corroborates the energy transfer from ZnSe QDs. However, in the case of the 1530 nm emission, a decrease of lifetime values suggests that the QDs might be acting as mediators in favoring energy migration among Er^{3+} ions, followed by non-radiative deactivation in lattice defects.

Credit author statement

The design and conduction of the experiment, the acquisition of data, the writing and modification of the paper are completed by Nilanjana Shasmal and Ana Candida Martins Rodrigues. Andrea Simone Stucchi de Camargo and Ana Candida Martins Rodrigues helped developing and perfecting the experimental ideas and technical route, also gave advices during the discussion of the experimental results.

Declaration of Competing Interest

The authors declare that they have no known competing financial interests or personal relationships that could have appeared to influence the work reported in this paper.

Data availability

No data was used for the research described in the article.

Acknowledgments

Authors would like to acknowledge the funding of this work by Fundação de Amparo a Pesquisa do Estado de São Paulo - FAPESP, through the Cepid Project No. 2013/07793-6 (CeRTEV – Center for Research, Technology and Education in Vitreous Materials). NS is particularly thankful to FAPESP for the postdoctoral fellowship (process No. 2018/04113-8). The authors would also like to thank Mr. Walter G. J. Faria for assisting with the spectroscopic measurements at LEMAF. The authors are also thankful to the infrastructure available at the Laboratory of Structural Characterization (LCE/DEMa/UFSCar).

Supplementary materials

Supplementary material associated with this article can be found, in the online version, at doi:10.1016/j.jnoncrysol.2023.122337.

References

[1] A.P. Alivisatos, Perspectives on the Physical Chemistry of Semiconductor Nanocrystals, J. Phys. Chem. 100 (1996) 13226.
[2] A.L. Rogach, L. Katsikas, A. Kornowski, Dangsheng Su, A. Eychmüller, H. Weller, Synthesis and characterization of thiol-stabilized CdTe nanocrystals, J. Phys. Chem. 100 (1996) 1772.
[3] V.I. Klimov, A.A. Mikhailovsky, S. Xu, A. Malko, J.A. Hollingsworth, C. A. Leatherdale, H.J. Eisler, M.G. Bawendi, Optical gain and stimulated emission in nanocrystal quantum dots, Science 290 (2000) 314.
[4] C.B. Murray, D.J. Norris, M.G. Bawendi, Synthesis and characterization of nearly monodisperse CdE (E= sulfur, selenium, tellurium) semiconductor nanocrystallites, J. Am. Chem. Soc. 115 (1993) 8706–8715.
[5] M. Gao, S. Kirstein, H. Möhwald, A.L. Rogach, A. Kornowski, A. Eychmüller, H. Weller, Strongly photoluminescent CdTe nanocrystals by proper surface modification, J. Phys. Chem. B 102 (1998) 8360–8363.
[6] X. Peng, L. Manna, W. Yang, J. Wickham, E. Scher, A. Kadavanich, A.P. Alivisatos, Shape control of CdSe nanocrystals, Nature 404 (2000) 59–61.
[7] L. Manna, D.J. Milliron, A. Meisel, E.C. Scher, A.P. Alivisatos, Controlled growth of tetrapod-branched inorganic nanocrystals, Nat. Mater. 2 (2003) 382–385.
[8] C. Dey, A.R. Molla, A. Tarafder, M. Mishra, G. De, M. Goswami, G. Kothiyal, B. Karmakar, Single-step in-situ synthesis and optical properties of ZnSe nanostructured dielectric nanocomposites, J. Appl. Phys. 115 (2014), 134309–1–134309-10.
[9] Qi Zhang, Huiqiao Li, Ying Ma, Tianyou Zhai, ZnSe nanostructures: synthesis, properties and applications, Prog. Mater. Sci. 83 (2016) 472–535.
[10] V.J. Leppert, S.H. Risbud, M.J. Fendorf, High-resolution electron microscopy and microanalysis of ZnSe quantum dots in glass matrices, Philos. Mag. Lett. 75 (2010) 29–34.
[11] Y. Wang, M. Wang, X. Yao, F. Kong, L. Zhang, Nonlinear optical absorption of ZnSe nanocrystals embedded in silica glasses, J. Cryst. Grow. 268 (2004) 575–579.
[12] Y. Wang, X. Yao, M. Wanga, F. Kong, J. He, Optical responses of ZnSe quantum dots in silica gel glasses, J. Cryst. Grow. 268 (2004) 580–584.
[13] N. Thantu, Second harmonic generation and two-photon luminescence upconversion in glasses doped with ZnSe nanocrystalline quantum dots, J. Lumin. 111 (2005) 17–24.
[14] P. Reiss, G. Quemarda, S. Carayon, J. Bleuse, F. Chandezon, A. Pron, Luminescent ZnSe nanocrystals of high color purity, Mater. Chem. Phys. 84 (2004) 10.
[15] M. Xia, C. Liu, Z. Zhao, B. Ai, Q. Yin, J. Xie, J. Han, X. Zhao, Formation and optical properties of ZnSe and ZnS nanocrystals in glasses, J. Non Cryst. Solid. 429 (2015) 79–82.
[16] C. Dey, M. Goswami, B. Karmakar, Structural and optical properties of ZnSe quantum dots in glass nanocomposites, Mater. Chem. Phys. 163 (2015) 554–561.
[17] G. Jose, G. Jose, V. Thomas, C. Joseph, M.A. Ittyachen, N.V. Unnikrishnan, Optical Characterization of Eu3+ Ions in CdSe Nanocrystal Containing Silica Glass, J. Fluoresc. 14 (2004) 733–738.
[18] Y. Yu, Y. Wang, D. Chen, P. Huang, E. Ma, F. Bao, Enhanced emissions of Eu3+ by energy transfer from ZnO quantum dots embedded in SiO2 glass, Nanotechnology 19 (2008), 055711.
[19] S. Mathew, P.R. Rejikumar, X. Joseph, N.V. Unnikrishnan, Optical studies on Eu3+/ZnSe nanocrystal in silica hosts, Opt. Mater. (Amst.) 29 (2007) 1689–1692.
[20] T.T. Van Tran, T.M. Dung Cao, Quang Vinh Lam, Van Hieu Le, Emission of Eu3+ in SiO2-ZnO glass and SiO2-SnO2 glass-ceramic: correlation between structure and optical properties of Eu3+ ions, J. Non Cryst. Solid. 459 (2017) 57–62.
[21] E.O. Serqueira, N.O. Dantas, Determination of the energy transfer section between CdS semiconductor quantum dots and Nd3+ ions, Opt. Mater. (Amst.) 90 (2019) 252–256.
[22] D. Chen, Y. Wang, E. Ma, F. Bao, Y. Yu, Luminescence of an Er3+-doped glass matrix containing CdS quantum dots, Scr. Mater. 55 (2006) 891–894.
[23] L. Bokatial, S. Rai, Structural and upconversion studies of Er3+ codoped with CdS nanoparticles in sol-gel glasses, J. Fluoresc. 22 (2012) 1639–1645.
[24] N. Shasmal, W.J. Faria, A.S.S. Camargo, A.C.M. Rodrigues, Enhancement in green and NIR emissions of Er3+ by energy transfer from ZnSe nanoparticles in borosilicate glass, J. Alloy. Compd. 863 (2021), 158428.
[25] N. Shasmal, W.J. Faria, A.S.S. Camargo, A.C.M. Rodrigues, Significant enhancement in Eu^{3+}/Eu^{2+} emissions intensity by CdS quantum dots, in chloroborosilicate glasses, J. Lumin. 243 (2022), 118623.
[26] C.L. Li, K. Nishikawa, M. Ando, H. Enomoto, N. Murase, Highly luminescent water-soluble ZnSe nanocrystals and their incorporation in a glass matrix, Colloid Surface A: Physicochem. Eng. Aspects 294 (2007) 33–39.
[27] P. Reiss, G. Quemarda, S. Carayon, J. Bleuse, F. Chandezon, A. Pron, Luminescent ZnSe nanocrystals of high color purity, Mater. Chem. Phys. 84 (2004) 10–13.

[28] C. Dey, M. Goswami, B. Karmakar, CdSe nanocrystals ingrained dielectric nanocomposites: synthesis and photoluminescence properties, Mater. Res. Express 2 (2015), 015014.
[29] C. Dey, A.R. Molla, Goswami M, G. Kothiyal, B. Karmakar, Synthesis and optical properties of multifunctional CdS nanostructured dielectric nanocomposites, J. Opt. Soc. Am. B 31 (2014) 1761.
[30] N. Shasmal, W.J. Faria, F.C. Serbena, A.S.S. Camargo, A.C.M. Rodrigues, Remarkable photoluminescence enhancement and tuning in Eu/CdS co-doped chloroborosilicate glass-ceramics, Ceram. Int. 48 (2022) 17196–17207.